Catalysis Today 176 (2011) 470–473

Contents lists available at ScienceDirect

Catalysis Today

journal homepage: www.elsevier.com/locate/cattod

Combustion of chlorinated VOCs using κ-$CeZrO_4$ catalysts

Beatriz de Rivas, Rubén López-Fonseca, Miguel Ángel Gutiérrez-Ortiz, José Ignacio Gutiérrez-Ortiz*

Chemical Technologies for Environmental Sustainability Group, Department of Chemical Engineering, Faculty of Science and Technology, Universidad del País Vasco/EHU, P.O. Box 644, E-48080 Bilbao, Spain

ARTICLE INFO

Article history:
Available online 10 November 2010

Keywords:
Chlorinated VOCs
Catalytic combustion
$Ce_{0.5}Zr_{0.5}O_2$ mixed oxide
Pyrochlores
Redox aging

ABSTRACT

In this work the application of a redox treatment consisting of a high temperature reduction with 5%H_2/Ar in the range 950–1075 °C for 3 h followed by mild oxidation at 550 °C with air was evaluated as a tool for improving the catalytic performance of $Ce_{0.5}Zr_{0.5}O_2$ mixed oxide in the combustion of 1,2-dichloroethane as a model chlorinated compound. Interestingly, after reduction at a temperature as high as 1050 °C, a substantially enhanced redox behaviour was noticed which resulted in a significant promotion of the catalytic activity in comparison with the unmodified parent sample. This active performance was assigned to the formation of a new κ-$CeZrO_4$ phase after redox aging characterised by a markedly increased capacity of providing active oxygen species at low temperatures.

1. Introduction

VOCs are wide ranging in chemical functionality and their emission sources (off-gases from chemical plants, groundwater decontamination by air stripping, odour emission control, and contaminated air in solvent evaporation processes) Particularly, chlorinated compounds require a special attention on account of their toxicity, high stability and widespread application in industry. Consequently, the discovery of efficient novel catalysts for low-temperature complete destruction of chlorinated VOCs is a challenging task of ongoing interest [1]. Previous studies carried out in our research group have shown promising results of the use of Ce/Zr mixed oxides for chlorinated VOCs oxidative decomposition [2]. The catalytic combustion is believed to chiefly involve redox catalysis with surface acidity playing a relevant catalytic role as well. In this work the impact of induced redox aging on the catalytic behaviour of $Ce_{0.5}Zr_{0.5}O_2$ was examined for the gas-phase catalytic destruction of chlorinated compounds. A characterisation study was undertaken to investigate the nature of the changes provoked. The comparative performance of fresh (calcined in air at 550 °C) and redox aged (reduced at 950–1075 °C for 3 h with 5%H_2/Ar followed by mild oxidation at 550 °C with 5%O_2/He for 0.5 h) samples was assessed using the oxidative destruction of 1,2-dichloroethane (DCE), which is a common chlorinated pollutant found in many commercial waste streams, in a fixed-bed flow reactor.

2. Experimental

2.1. Catalyst preparation and characterisation

The original $Ce_{0.5}Zr_{0.5}O_2$ sample was synthesised by Rhodia using a proprietary coprecipitation method (precipitation route from nitrate precursors). This sample was stabilised by calcination in air at 550 °C for 4 h in a muffle furnace (fresh sample denoted as CZ(550)). The redox aging consisted of a reduction step under flowing 5%H_2/Ar (50 cm^3 min^{-1}) at temperatures in the 950–1075 °C range for 3 h. After cooling in a flow of helium (50 cm^3 min^{-1}) down to 550 °C the sample was reoxidised under flowing oxygen (5%O_2/He, 50 cm^3 min^{-1}) for 0.5 h. The treated samples were labelled as follows CZ(950), CZ(1000), CZ(1050), and CZ(1075).

Textural properties were evaluated from the nitrogen adsorption–desorption isotherms, determined at −196 °C with a Micromeritics ASAP 2010 apparatus. Structural properties were evaluated by X-ray diffraction (X'PERT-MPD X-ray diffractometer) and Raman spectroscopy (Renishaw InVia Raman spectrometer coupled to a Leica DMLM microscope). Acid properties were determined by temperature-programmed desorption (TPD) of ammonia. The redox behaviour was examined by temperature-programmed reduction (TPR) with hydrogen. For both TPD and TPR analysis a Micromeritics AutoChem 2920 instrument coupled to a thermal conductivity detector was used. Finally, oxygen storage capacity (OSC) measurements at 400 °C were carried out on a Micromeritics ASAP 2010 apparatus.

2.2. Catalyst activity determination

Catalyst behaviour over the range 200–550 °C was determined using a lab-scale fixed-bed reactor, in which typically 0.85 g of cat-

* Corresponding author. Tel.: +34 94 6012683; fax: +34 94 6015963.
E-mail address: joseignacio.gutierrez@ehu.es (J.I. Gutiérrez-Ortiz).

0920-5861/$ – see front matter © 2010 Elsevier B.V. All rights reserved.
doi:10.1016/j.cattod.2010.10.044

Table 1
Physico–chemical properties of $Ce_{0.5}Zr_{0.5}O_2$ samples.

Catalyst	BET surface area, $m^2\,g^{-1}$	Pore volume, $cm^3\,g^{-1}$	Average pore size, Å	Total acidity, μmol $NH_3\,g^{-1}$	H_2 consumption, μmol g^{-1} (650 °C)	% Reduction (650 °C)	O_2 consumption, μmol g^{-1} (400 °C)
CZ(550)	99	0.21	65	232	1210	71	153
CZ(950)	24	0.11	210	105	1623	96	320
CZ(1000)	19	0.08	240	98	1709	100	390
CZ(1050)	10	0.03	330	53	1723	100	437
CZ(1075)	11	0.02	350	43	1730	100	576

alyst (0.3–0.5 mm) was loaded [3]. The reaction feed consisted of 1000 ppm of DCE in dry air. A total flow rate of 500 $cm^3\,min^{-1}$ was used and catalysts were packed to a constant volume to give a gas hourly space velocity of 30,000 h^{-1}. The feed and effluent streams were analysed using an on-line 7980A Agilent Technologies gas chromatograph equipped with a thermal conductivity (CO and CO_2) and an electron capture detector (chlorinated hydrocarbons). Analysis of HCl and Cl_2 was carried out by means of an ion selective electrode and titration, respectively. Further details on analytical procedures are described elsewhere [3].

3. Results

3.1. Characterisation of $Ce_{0.5}Zr_{0.5}O_2$ samples

The starting $Ce_{0.5}Zr_{0.5}O_2$ sample was a mesoporous solid with a surface area of 100 $m^2\,g^{-1}$, a BJH average pore diameter of 64 Å and a total pore volume of 0.21 $cm^3\,g^{-1}$. As shown in Table 1 the treatment at high temperatures provoked a progressive drop in the surface area (10–11 $m^2\,g^{-1}$) and pore volume (0.02–0.03 $cm^3\,g^{-1}$) along with a significative increment in the pore size (300–350 nm) [4]. Fig. 1 showed the XRD patterns of fresh and thermally treated $Ce_{0.5}Zr_{0.5}O_2$ samples. The pattern of the fresh sample presented broad reflections corresponding to the tetragonal t′ phase. It is known that reduction at high temperatures of a starting t′-($Ce_{0.5}Zr_{0.5}O_2$) phase leads to an ordered pyrochlore-type $Ce_2Zr_2O_{7+\delta}$ structure, in which the cations are arranged in a face centred cubic structure but are ordered along the 1 1 0 direction. When the pyrochlore is submitted to a mild oxidation step the ideal κ-$CeZrO_4$ phase can be obtained [5]. The powder X-ray diffraction pattern of the pyrochlore-type precursor is composed of the fundamental diffraction for the CaF_2-type structure and additional peaks assigned to the ordered arrangement of cations. As shown in Fig. 1 after reduction at >1050 °C, distinct diffraction peaks (marked with an asterisk, and not present in the parent sample) corresponding to the κ-$CeZrO_4$ phase were noticeable at 2θ 14°, 28°, 36°, 45°, 52°, 63° and 68° [6,7]. Intensities of these additional peaks in the XRD patterns were relatively small and broad. This was attributed to incomplete cation ordering, giving rise to antiphase domain boundaries, as pointed out by Moriga et al. [8].

Raman spectra of the treated $Ce_{0.5}Zr_{0.5}O_2$ samples are collected in Fig. 2. The spectrum of the base/reference sample is dominated by an intense peak at 465 cm^{-1} characteristic of the fluorite. Two less prominent bands near 625 and 300 cm^{-1} were also noticeable as well. Such a spectral feature was attributed to the presence of a t′ phase, which is a tetragonal phase with the axial ratio a/c equal to 1 [9]. In contrast, the Raman spectra of the redox aged samples showed a large number of peaks. The strongest signals, located at 271, 440 and 596 cm^{-1}, were assigned to the κ-phase [5,10]. For the κ-phase obtained after reduction at increasing temperatures, the peaks became narrower and more intense. In line with the XRD results, it could be concluded that, in the presence of a concentration of 5%H_2, 1050 °C was a sufficiently high reduction temperature to induce cation ordering. Acid properties were evaluated by means of NH_3-TPD. It was found that the area under the TPD curves dropped significantly for all redox oxides compared with the fresh sample, thereby showing an overall loss of the total number of acid sites (45–80%) with increasing temperature.

On the other hand, the redox properties of ceria-containing materials were investigated by temperature-programmed reduction with hydrogen and by measuring the oxygen storage capacity. The TPR profiles of fresh and redox aged samples are included in Fig. 3. The fresh sample shows a single broad reduction centred about 550 °C, which was related to the concurrent surface and bulk reduction. It is widely accepted that insertion of ZrO_2 into the cubic CeO_2 resulted in a distortion on the mixed oxide which allowed for a higher mobility of the lattice oxygen [11]. In spite of the sintering process that takes place during the pre-treatment the redox behaviour of the resulting samples was indeed markedly modified and enhanced in two ways in comparison with the starting tetragonal phase [12]. On one hand, the consumption of H_2 was appreciably accelerated since it started at about 325 °C compared with 400 °C for the fresh sample. A second reduction peak was additionally observed at slightly lower temperatures, about 525 °C. On the other hand, the overall H_2 uptake at 650 °C was significantly increased

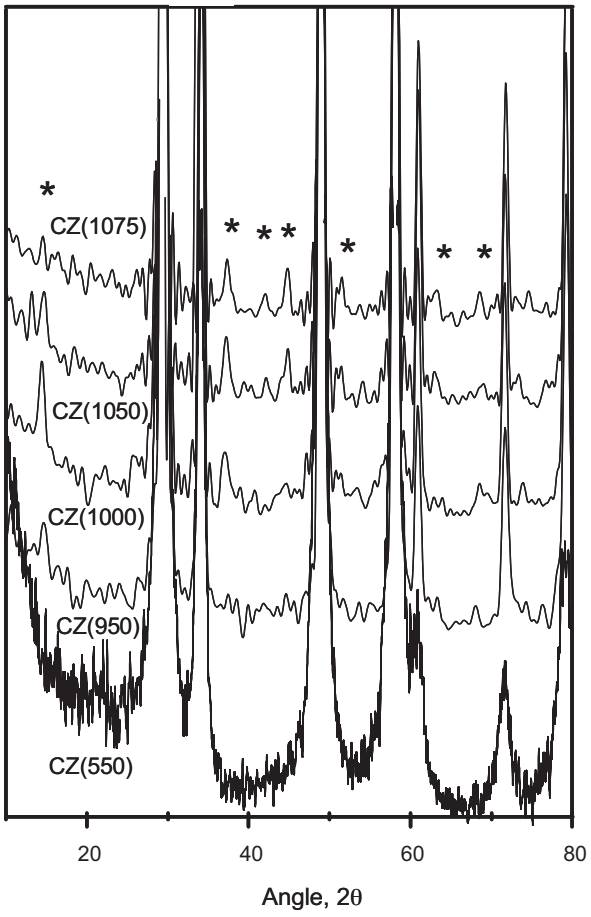

Fig. 1. XRD diffraction patterns of $Ce_{0.5}Zr_{0.5}O_2$ samples.

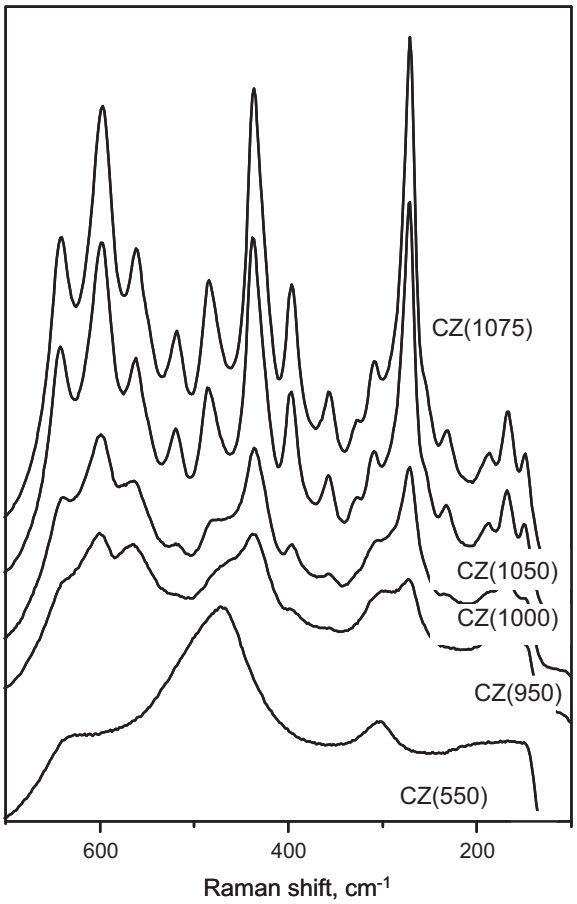

Fig. 2. Raman spectra of the $Ce_{0.5}Zr_{0.5}O_2$ samples.

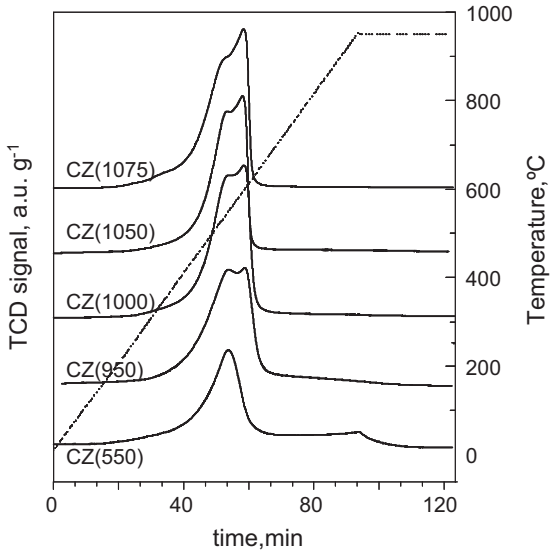

Fig. 3. H_2-TPR profiles of the $Ce_{0.5}Zr_{0.5}O_2$ samples.

from 1.21 for the reference sample up to 1.73 mmol H_2 g^{-1} for CZ(1075) sample. The better redox behaviour of the κ-$CeZrO_4$ sample was associated with the enhancement of the homogeneity of the Ce and Zr atoms that could ease the valance change of the Ce. This modification of the local environment around Ce and Zr will generate some active oxygen species for the promotion of the redox behaviour [13].

O_2 uptake or oxygen storage capacity can be taken as a measure of the amount of oxygen vacancies created upon reduction [12]. This is an interesting parameter to discuss on the basis of labile oxygen for the reaction since it represents how much oxygen will be available for the oxidation of the chlorinated feed. Table 1 lists the OSC values at 400 °C. It was noted that OSC was markedly greater for the cation-ordered samples with respect to the fresh sample. Also marked differences were observed among the redox aged samples. Hence OSC for CZ(1075) was 576 μm O_2 g^{-1} compared with 437, 390 and 320 μm O_2 g^{-1} for CZ(1050), CZ(1000) and CZ(950) samples, respectively.

3.2. Catalytic behaviour of $Ce_{0.5}Zr_{0.5}O_2$ samples

The activity for DCE oxidation in terms of T_{50} and T_{90} values (temperatures required to attain 50 and 90% conversion, respec-

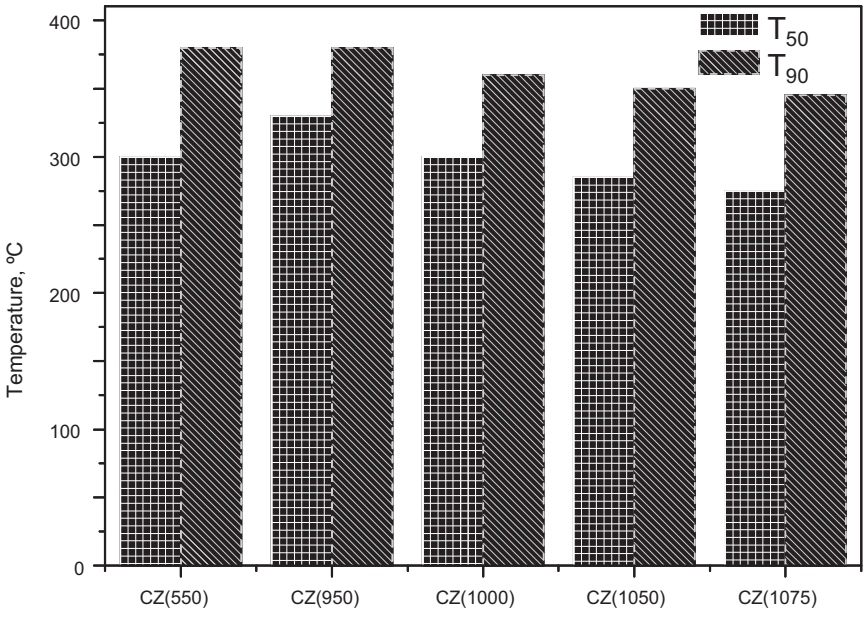

Fig. 4. Activity of the $Ce_{0.5}Zr_{0.5}O_2$ samples in the oxidation of DCE.

tively) are reported in Fig. 4. Taking the performance of CZ(550) sample as a reference two different behaviours were noticed for the redox aged samples. The first set of samples, including those reduced at 950 and 1000 °C, showed a lower activity. In contrast, an increase in conversion was noted for those oxides that were reduced at a temperature higher than 1050 °C. Hence, the light-off temperature of half conversion decreased from 300 over the fresh sample down to 285 and 275 °C over CZ(1050) and CZ(1075), respectively. Although the samples reduced at lower temperatures also exhibited promoted redox properties, it was interpreted that this improvement was not sufficient to reveal a better catalytic activity. Note that the transformation into a pyrochlore structure was not successfully attained under these conditions as evidenced by Raman spectroscopy and XRD. In other words, the combination of moderate redox properties with a significant total acidity found in the starting sample (CZ(550)) sample resulted in a more catalytically active mixed oxide. On the contrary, the better behaviour of the samples reduced at 1050–1075 °C was attributed to their greater capability of providing active oxygen species at low temperatures which overcompensated for the loss of acidity and surface area.

4. Conclusions

The application of controlled redox aging for $Ce_{0.5}Zr_{0.5}O_2$ mixed oxide appears to be an efficient strategy for improving its performance for chlorinated VOC removal. Although the thermally treated materials sintered to a notable degree and exhibited remarkably low surface areas, the formation of catalytically active samples was evidenced upon application of a reduction temperature higher than 1050 °C. Compared with the starting material these samples accelerated the oxidative destruction of the selected model chlorinated compound. Pyrochlore-type ordering in the cation sublattice (κ phase) with improved oxygen mobility at low temperatures was responsible for this enhanced catalytic performance. Among the redox conditions examined reduction at 1075 °C for 3 h, which led to a more homogeneous ordered arrangement of cations, resulted in the most active sample with an advance in the reaction temperature of 25 °C.

Acknowledgements

The authors wish to thank the UPV/EHU-Gobierno Vasco (SAIOTEK S-PE09UN23) for the financial support.

References

[1] J.J. Spivey, in: G. Ertl (Ed.), Handbook of Heterogeneous Catalysis, vol. 5, Wiley-VCH, Verlag Weinheim, 2008, pp. 2394–2411.
[2] J.I. Gutiérrez-Ortiz, B. de Rivas, R. López-Fonseca, J.R. González-Velasco, Appl. Catal. A 269 (2004) 147–155.
[3] R. López-Fonseca, S. Cibrián, J.I. Gutiérrez-Ortiz, M.A. Gutiérrez-Ortiz, J.R. González-Velasco, AIChE J. 49 (2003) 496–504.
[4] P. Fornasiero, T. Montini, M. Graziani, J. Kaspar, A.B. Hungría, A. Martínez-Arias, J.C. Conesa, Phys. Chem. Chem. Phys. 4 (2002) 149–159.
[5] T. Omata, H. Kishimoto, S. Otsuka-Yao-Matsuo, N. Ohtori, N. Umesaki, J. Solid State Chem. 147 (1999) 573–583.
[6] Z. Hui, N. Guillet, F. Valdivieso, M. Pijolat, Solid State Ionics 160 (2003) 317–326.
[7] T. Montini, N. Hickey, P. Fornasiero, M. Graziani, M.A. Bañares, M.V. Martínez-Huerta, I. Alessandri, L.E. Depero, Chem. Mater. 17 (2005) 1157–1166.
[8] T. Moriga, S. Emura, A. Yoshiasa, S. Kikkawa, F. Kanamaru, K. Koto, Solid State Ionics 40–41 (1990) 357–361.
[9] T. Masui, K. Nakano, T. Ozaki, G. Adachi, Z. Kang, L. Eyring, Chem. Mater. 13 (2001) 1834–1840.
[10] S. Otsuka-Yao-Matsuo, T. Omata, N. Izu, H. Kishimoto, J. Solid State Chem. 138 (1998) 47–54.
[11] J.I. Gutiérrez-Ortiz, B. de Rivas, R. López-Fonseca, J.R. González-Velasco, Catal. Today 107–108 (2005) 933–941.
[12] H. Vidal, J. Kaspar, M. Pijolat, G. Colon, S. Bernal, A. Cordón, V. Perrichon, F. Fally, Appl. Catal. B 27 (2000) 49–63.
[13] Y. Nagai, T. Yamamoto, T. Tanaka, S. Yoshida, T. Nonaka, T. Okamoto, A. Suda, M. Sugiura, Catal. Today 74 (2002) 225–234.